

Photoelectron spectroscopy of HCCS radical

M. Drissi,¹ G. A. Garcia,² B. Gans,³ S. Boyé-Péronne,³ H. R. Hrodmarsson,⁴ L. Nahon,² and J.-C. Loison⁵

¹*Synchrotron SOLEIL, L'Orme des Merisiers, Départementale 128, 91190 Saint-Aubin, France.*

²*Synchrotron SOLEIL, L'Orme des Merisiers, St. Aubin BP 48, 91192 Gif sur Yvette, France.*

³*Institut des Sciences Moléculaires d'Orsay (ISMO), CNRS, Université Paris-Saclay, 91405 Orsay, France.*

⁴*Univ Paris Est Creteil and Université Paris Cité, CNRS, LISA, F-94010 Créteil, France.*

⁵*Institut des Sciences Moléculaires (ISM), CNRS, Univ. Bordeaux, 351 cours de la Libération, Talence, 33400, France.*

(*Electronic mail: jean-christophe.loison@cnrs.fr)

(*Electronic mail: myriam.drissi@synchrotron-soleil.fr)

(Dated: 3 February 2026)

Linear carbon chains are an important family of molecules detected in various astrophysical environments. In this work, we investigate the vacuum ultraviolet photoionization of HCCS, the smallest sulfur-bearing carbon chain in the HC_nS family. The radical is produced from thiirane *in situ* in a flow-tube reactor coupled to a microwave discharge. The vibronic structures are assigned using *ab initio* calculations. The adiabatic ionization energies toward the ground ($X^+ \ ^3\Sigma^-$) and first electronic excited ($a^+ \ ^1\Delta$) states of the cation are measured experimentally for the first time at 9.191 ± 0.003 eV and 9.856 ± 0.003 eV, respectively, while a tentative value of 10.364 ± 0.006 eV is offered for the $b^+ \ ^1\Sigma^+$ state.

I. INTRODUCTION

The thioketenyl radical (HCCS) is the smallest sulfur-bearing carbon chain in the HC_nS family. It has been detected in both its neutral and cationic forms in the Taurus molecular cloud TMC-1.^{1,2} This discovery is part of a broader trend, as numerous carbon chain molecules have been observed in the interstellar medium (ISM). This includes not only pure carbon chains but also the ones incorporating heteroatoms such as nitrogen, oxygen, and sulfur, as well as metal-like magnesium and metalloid-like silicon. Such molecules are observed in diverse astrophysical environments, including star-forming regions, protoplanetary disks, young stellar objects (YSOs), and external galaxies, highlighting the ubiquity of this molecular family.³ Among these objects, low-mass and high-mass YSOs are found to exhibit distinct chemical differentiation during their formation process, leading to regions enriched either in carbon chains or in complex organic molecules (COMs). Several factors have been proposed to drive this differentiation, including temperature, the intensity of the radiation field, and the impact of cosmic rays; however, their relative contributions remain uncertain.^{4–6} In the case of low-mass YSOs, Spezzano *et al.*⁷ suggested that variations in the far-ultraviolet component of the interstellar radiation field could play a key role. This hypothesis is supported by theoretical results from two different models,^{8,9} both indicating a potential link between far ultra-violet radiation and the observed chemical diversity.

In this context, the study of carbon chains exposed to vacuum ultra-violet (VUV) radiation is of interest to extract key information such as ionization energies (IE), cation fragmentation onsets and photoionization cross-sections. On a more fundamental point of view, such an interaction allows extracting spectroscopic information which is needed to benchmark

theoretical models. These data can also be used to identify and quantify reaction products in laboratory experiments,¹⁰ thereby contributing to the refinement of our understanding of sulfur chemistry, where models sometimes show discrepancies with observed molecular abundances.^{1,2}

The electronic structure of HCCS has been extensively investigated as a prototypical tetra-atomic linear molecule with a $^2\Pi$ electronic ground state, which exhibits a Renner–Teller effect. Both experimental^{11–21} and theoretical^{22–31} studies have contributed to our understanding of this system. In contrast, the HCCS⁺ cation has only been characterized theoretically. Initial studies employed Hartree–Fock and Møller–Plesset perturbation theory, predicting a $^3\Sigma^-$ electronic ground state for the cation.³² Later, Puzzarini³³ conducted a more comprehensive investigation using the CCSD(T) method. This work examined the neutral, cationic, and anionic species of HCCS, reporting adiabatic ionization energies (IEs) of 9.114 eV and 9.958 eV towards the ground and first electronic excited states of the cation, respectively. Additionally, the study provided equilibrium geometries, dipole moments, and electron affinity values. To the best of our knowledge, no experimental data are currently available for HCCS⁺. In the present work, H-abstraction reaction in a flow tube reactor with thiirane ($\text{c-C}_2\text{H}_4\text{S}$) is employed to produce the HCCS radical. Using VUV synchrotron radiation in the 8.5 – 11.0 eV region and the threshold photoelectron spectroscopy (TPES) technique, we have measured for the first time the photoelectron spectroscopy of this radical.

During the review process of this article, a study on HCCS⁺ has been published by Michielan *et al.*³⁴ presenting its infrared action spectrum between 450–1850 cm^{-1} and 3000–3350 cm^{-1} allowing assignment of vibrational bands for both the triplet and the singlet lowest states of the cation.

II. METHOD

A. Experimental

Experiments were performed using a flow tube reactor coupled to a microwave (MW) discharge installed inside the permanent endstation SAPHIRS³⁵ on the undulator-based DESIRS beamline at the SOLEIL synchrotron.³⁶ The setup has been described in detail elsewhere and will be only outlined briefly here.³⁷

The flow-tube is composed of a main tube reactor and a collinear sliding injector. Fluorine atoms are produced by MW discharge of a mixture of F₂ (Air liquide 5% in He) and He (Air liquide 99.995%) which is fed into the main reactor. The precursor, thiirane (c-C₂H₄S) (Sigma-Aldrich 98%), is kept at -20°C inside a thermostated bath. A needle valve is used to adjust the precursor density fed into the injector. The reaction time between fluorine atoms and thiirane is controlled by adjusting the position of the injector inside the reactor. The total pressure in the reactor is 6.5×10^{-1} mbar for a total flow of around 1000 sccm (standard cubic centimeter per minute). The concentrations of fluorine and thiirane are estimated to be around 1×10^{13} and 3×10^{13} cm⁻³, respectively. The F atoms can react with the precursor and abstract three H atoms to generate the HCCS molecule. The experimental conditions, including precursors concentration and injector distance, are optimised to get the best signal-to-background ratio. A mass spectrum of the reactor content is provided in supplementary information.

The reactor content is skimmed twice before entering the ionization chamber where it crosses the linearly polarized VUV synchrotron beam with a right angle in the center of the DELICIOUS III spectrometer.³⁸ A gas filter,³⁹ located upstream is filled with krypton to ensure a high spectral purity, removing the harmonics from the undulator spectrum. The resulting electrons and ions are accelerated in opposite direction by a $F = 88$ V·cm⁻¹ electric field toward a velocity map imaging (VMI) and a Wiley-McLaren time-of-flight (TOF) analyzer, respectively. The data are sorted into correlated pairs by means of a PEPICO acquisition scheme and allows the multiplexed recording of mass-selected photoelectron images. The extraction field used to separate the particles induces a downshift of the ionization energies of 7 meV, following the well-established formula $6\sqrt{F}$ (cm⁻¹).⁴⁰ All values given below were shifted up accordingly.

The spectrum was recorded by scanning the photon energy between 8.9 and 11 eV with a 6 meV step, and were normalized by the recorded photon flux based upon a Si photodiode measurement. The absolute energy calibration was achieved with the atomic sulfur ionization energy, the sulfur sharp autoionization features between 10.59 and 10.73 eV, and the Kr 4p⁵ 5s (3/2) and 4p⁵ 5s (1/2) absorption lines from the gas filter. This led to an absolute energy scale accuracy of 3 meV over the full energy range. The photon resolution was set to 0.72 Å (6 meV at 10 eV). The total (electron + photon) energy resolution was measured at 14 meV from the atomic signals.

The ion image was used to select a "Region of Interest" corresponding solely to ions possessing a velocity component

along the molecular beam axis, therefore removing the contribution from species not originating from the flow tube reactor, discarding contributions from the ionization chamber background (as previously described³⁷). Furthermore, the ion image analysis provided an estimation of the translational temperature of around 300 K, which is assumed equal to the rotational temperature.⁴¹

B. Computational

The Franck-Condon (FC) factors for photoionization were calculated using the ezSpectrum software⁴² with geometry optimization and harmonic frequency calculations performed at the DFT level applying the M06-2X functional and the AVTZ basis set using Gaussian 2016 Software.⁴³ The harmonic approximation was applied for harmonic frequencies and normal modes in both the neutral and the cationic ground states and the Condon approximation was applied for the dipole moment. The Duschinsky effect was considered using recursive formulae already implemented in the ezSpectrum. The potential energy curves of the two lowest electronic states of HCCS and the four lowest electronic states of HCCS⁺ were computed as a function of the H-C-CS angle (all other parameters being optimized) using the AVTZ basis set and MOLPRO 2015 package.⁴⁴ The *ab initio* calculations on the electronic states were carried out using the internally contracted multireference configuration interaction method with the Davidson correction (MRCI + Q) and complete active space self-consistent field (CASSCF) wave functions. The CASSCF and MRCI calculations were performed with 7 (6 for HCCS⁺) electrons distributed in 7 orbitals.

III. RESULTS AND DISCUSSION

The mass-selected photoelectron spectrum (PES) matrix of HCCS (*m/z* 57) between 8.9 and 11 eV is displayed in figure 1. Such matrix is built by performing the Abel transformation on the electron image to extract the electron kinetic energy for each photon energy. A wealth of information can be extracted from this 2D matrix. For instance, the ion yield can be obtained by integrating the total signal at each photon energy, as presented in white in figure 1. Some sharp features, assigned to autoionizing Rydberg states, can be observed on this ion yield, however, their exact assignment is beyond the scope of this article. Another way to reduce this matrix is by integrating the photoelectron signal along constant ionic state lines, a method described by Pouilly *et al.*⁴⁵, yielding the so-called slow photoelectron spectrum (SPES). In this work, only slow electrons with kinetic energies up to 50 meV were considered; therefore, all resulting spectra will be referred to as threshold photoelectron spectrum (TPES) throughout this article.

As discussed in the introduction, previous studies have shown that the X ²Π ground state of HCCS has a linear geometry.¹¹ Consequently, two effects will split the ground state energy: the Renner-Teller effect and spin-orbit coupling. In the case of the neutral ground state, the Ren-

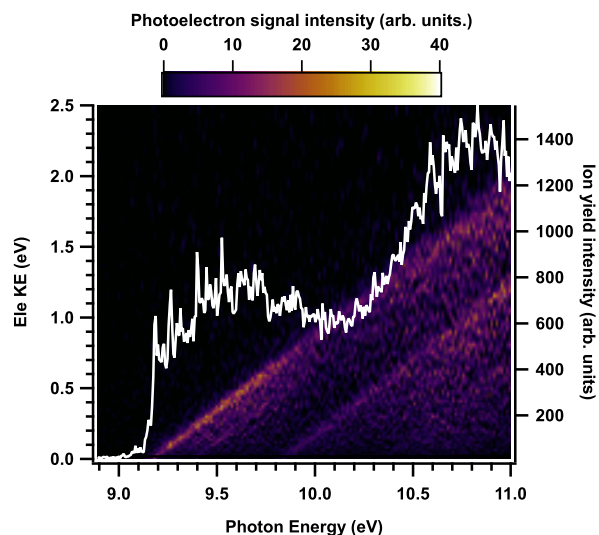


FIG. 1: Mass-selected photoelectron signal as a function of the photon energy (horizontal axis) and the electron kinetic energy (vertical axis), for m/z 57. The ion yield, obtained by integrating the signal over all electron energies, is represented on top of the matrix by a white solid line.

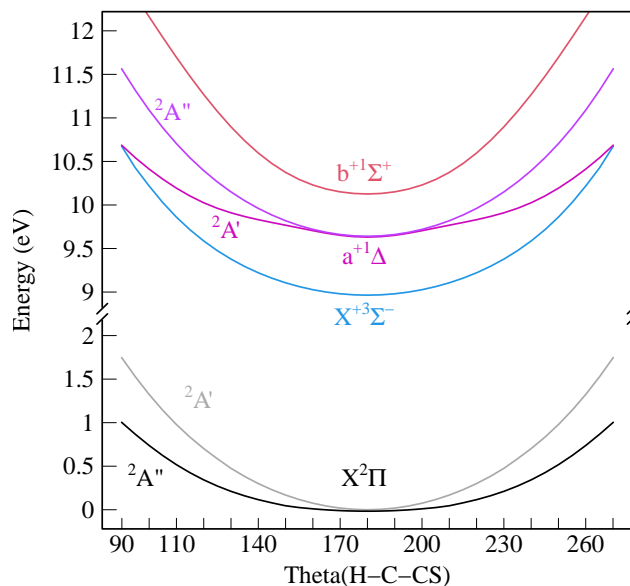


FIG. 2: Cut in the potential energy surfaces of the HCCS and HCCS⁺ molecules as a function of the H-C-CS bending angle calculated at the MRCI+Q/AVTZ level. The other distances and angles were optimized.

ner-Teller effect lowers the linear symmetry to C_s and splits the state into two components, $^2A''$ and $^2A'$, along the H-C-C bending coordinate (see Figure 2). Additionally, spin-orbit coupling further splits the $^2\Pi$ state into $\Omega = 1/2$ and $\Omega = 3/2$ components, with the $3/2$ component lying lower in energy ($A_{SO} = -276.56 \text{ cm}^{-1}$).¹³ Assuming the available thermal energy equals the translational temperature determined from the

ion image, the population ratio between the two spin-orbit components is estimated to be 0.3. As a result, the ionizing transition is expected to originate predominantly from the $X^2\Pi_{3/2}$ state, although we note that the above assumption of thermal equilibrium is not correct, as shown by the much higher vibrational temperature extracted from the vibrational branching ratios in the TPES. The mass-selected TPES of m/z 57 is shown in Figure 3, together with the simulated spectra which origins has been determined to best reproduce the experimental trace. Since the HCCS ground state and HCCS⁺ first excited electronic state are affected by the Renner-Teller effect, a FC simulation may be insufficient to fully reproduce the observed spectral structure, due to the breakdown of the Born-Oppenheimer approximation. Nevertheless, in this case the simple FC calculation with a vibrational temperature of 1000 K already shows good agreement with the experimental spectrum.

Comparison with the *ab initio* calculation allows the identification of two origin bands: the first at $9.191 \pm 0.003 \text{ eV}$ and the second at $9.856 \pm 0.003 \text{ eV}$. These, together with the computed values, are summarized in Table I. Each of the origin bands presents a shoulder on the left side which is well reproduced in the simulation using the SO constant derived by He and Clouthier ($A_{SO} = -276.56 \text{ cm}^{-1} = 34.3 \text{ meV}$)¹³ and our estimated SO-component population ratio. The relative ionization efficiency of each photoionization transition can be estimated as detailed in our prior work.⁴⁶ Briefly, the relative photoionization efficiency for each transition is estimated considering only transitions involving the ejection of a single electron and assuming similar electronic wavefunction overlaps. In the case of HCCS the neutral electronic ground state has an electronic configuration equal to $(1-9)\sigma^2(1-2)\pi^43\pi^3$ and the three lowest electronic states of HCCS⁺, accessible by direct ionization, are all issued from the $(1-9)\sigma^2(1-2)\pi^43\pi^2$ electronic configuration. The probability of the photoionizing transition is, in our simplified approximation, proportional to the weight product of the initial and final main configurations involved in single electron ionization processes, times the degeneracy of the projection of the orbital angular momenta and the spin multiplicities of the initial and final electronic states. The relative photoionization intensities from HCCS($X^2\Pi$) toward HCCS⁺ in the $X^+3\Sigma^-/a^+1\Delta/b^+1\Sigma^+$ states are then equal to 3/2/1. These theoretical intensities are in qualitative agreement with the observed intensities. However, it should be noted that photoionization to the HCCS⁺ ($X^+3\Sigma^-$) ground state is clearly favored, likely due to the presence of autoionization resonances which are known to affect the relative intensities of the TPES peaks.⁴⁷ Indeed, these resonances are clearly seen in the total ion yield spectra shown in Figure 1.

The measured adiabatic ionization energy (AIE) of $9.191 \pm 0.003 \text{ eV}$ can be assigned to the $X^+3\Sigma^- \leftarrow X^2\Pi_{3/2}$ ionizing transition and is in reasonable agreement with the computed value of 9.114 eV reported by Puzzarini³³ and with our calculations (8.90 eV at M06-2X/AVTZ level and 9.00 eV at MRCI+Q/CBS with geometry and ZPE calculated at AVTZ level). According to our calculations, the vibrational structure in the TPES arises mainly from the ν_2^+ and ν_3^+ modes, corre-

sponding to the C-C and C-S stretching modes, respectively. The observed peaks are assigned to the adiabatic transition, the v_2^+ and v_3^+ fundamentals and the $v_2^+ + v_3^+$ combination band. The observed frequencies for the v_2^+ and v_3^+ modes, $1701 \pm 48 \text{ cm}^{-1}$ and $871 \pm 48 \text{ cm}^{-1}$ respectively, show good agreement with the work of Michielan *et al.*³⁴. In particular, the v_2^+ frequency is in agreement with their experimental value, and both modes are consistent with the theoretical frequencies reported therein. Note that the mode numbering used here follows the notation of He and Clouthier¹¹ and differs from that adopted by Michielan *et al.*³⁴.

The second electronic band corresponds to the $a^+ {}^1\Delta \leftarrow X {}^2\Pi_{3/2}$ ionizing transition, where the final state is expected to undergo Renner–Teller splitting into two components as shown in figure 2. Here, both states are linear with a small geometry change. However, the Renner-Teller effect will probably affect the vibrational structure along the RT active modes (v_4 and v_5 bending modes), although we have not observed any RT signature in our TPES. In this band, due to the lower signal-to-background from the abovementioned statistical arguments, only the adiabatic transition could be fitted, resulting in an AIE of $9.856 \pm 0.003 \text{ eV}$. This value is significantly lower than the value calculated by Puzzarini³³ for the first singlet electronic state of HCCS^+ , 9.958 eV , labelled ${}^1\Sigma^+$ state in their paper, probably due to an unsuitable choice for the reference determinant, or the multi-reference nature of this molecule. The experimental value is also significantly lower than calculated at the M06-2X/AVTZ level, equal to 10.21 eV . This theoretical overestimation of the IE is likely due to the multi-configurational aspect of the $a^+ {}^1\Delta$ electronic state of HCCS^+ . The multiconfiguration MRCI+Q/CBS method gives slightly better results, 9.68 eV , but underestimates the IE value, as in the case of ionization to the ground state of HCCS^+ . Finally, we note that the recent experimental study by Michielan *et al.*³⁴ reports an energy separation of 0.23 eV (22 kJ/mol) between the ground state and the first excited state of HCCS^+ , which is inconsistent with the TPES measurements (0.665 eV) and the calculation (0.68 eV) presented here.

The weak signal peaking at 10.364 eV in the TPES may be due to the photoionization toward the second excited state $b^+ {}^1\Sigma^+ \leftarrow X {}^2\Pi$ calculated at 10.16 eV at the MRCI+Q/CBS level, thus with a similar red shift of around -0.2 eV than the MRCI+Q/CBS calculations for $X^+ {}^3\Sigma^- \leftarrow X {}^2\Pi_{3/2}$ and $a^+ {}^1\Delta \leftarrow X {}^2\Pi_{3/2}$ ionizing transitions. In addition, its relative intensity is consistent with our statistical estimate, *i.e.*, twice as weak as the $a^+ {}^1\Delta \leftarrow X {}^2\Pi$ ionizing transition. We therefore tentatively associate an adiabatic ionization energy of $10.364 \pm 0.006 \text{ eV}$ to the $b^+ {}^1\Sigma^+$ state, but we note that the low signal-to-background precludes a categorical assignment. For this reason, this AIE is not included in Table I.

IV. CONCLUSIONS

The thioketenyl radical photoelectron spectrum has been recorded in the region of the ground and first excited state for the first time using a double imaging photoelectron photoion spectrometer. HCCS was produced through H abstractions

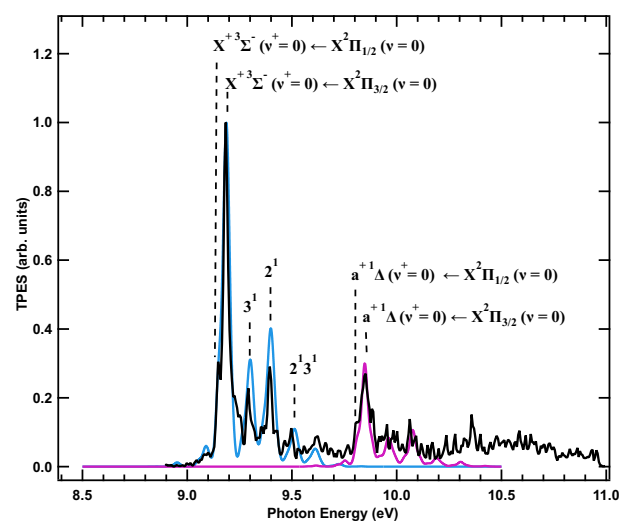


FIG. 3: Mass-selected experimental TPES of HCCS in the vicinity of $X^+ {}^3\Sigma^- \leftarrow X {}^2\Pi$ and $a^+ {}^1\Delta \leftarrow X {}^2\Pi$ ionizing transitions (black trace) compared to Franck-Condon simulations performed with $T_{\text{vib}} = 1000 \text{ K}$ (blue and pink traces, respectively). The relative intensities of the simulations have been adjusted to reproduce the experimental trace. The origins of the FC simulations have been determined as the best match to our experimental TPES. The vibrational assignments follow the usual notation, where the mode index is given by the main number and the superscript indicates the number of quanta excited in that mode, and they all correspond to the $X^+ {}^3\Sigma^- \leftarrow X {}^2\Pi_{3/2}$ band.

of thiirane with fluorine atoms in a discharge flow-tube reactor. The two intense vibronic bands were assigned with the aid of *ab initio* calculations, yielding the adiabatic ionization energies. The first excited state was determined to be ${}^1\Delta$, in contrast to earlier calculations that assigned it as ${}^1\Sigma^+$. This work is the first experimental determination of the adiabatic ionization energies of HCCS. These data provide a foundation for use in thermochemical calculations, such as determining the enthalpy of formation or the dissociation energy of the cation.⁴⁸ However, since the corresponding thermochemical parameters of the neutral species remain unknown, their determination is necessary before these derived quantities can be accurately evaluated. In addition, the photoelectron spectrum acts as a fingerprint that can be used to detect HCCS in advanced mass spectrometry experiments in gas phase reaction studies.¹⁰ Finally, it is worth noting that experimental values are still needed to benchmark theoretical methods, where even for relatively small systems what many consider the gold standard (CCSD(T)) fails, and multireference/multiconfigurational methods are off by 0.2 eV .

V. SUPPLEMENTARY ONLINE MATERIAL

See the supplementary material for the TOF mass spectrum of the reactor content.

	EXP	M06-2X/AVTZ	MRCI+Q/CBS	CCSD(T) ³³
$X^+ \ ^3\Sigma^- \leftarrow X \ ^2\Pi_{3/2}$	9.191 ± 0.003	8.90	9.00	9.114
$a^+ \ ^1\Delta \leftarrow X \ ^2\Pi_{3/2}$	9.856 ± 0.003	10.21	9.68	9.958
$b^+ \ ^1\Sigma^+ \leftarrow X \ ^2\Pi_{3/2}$	-	-	10.16	-

TABLE I: Experimental and calculated ionization energies in eV of HCCS in the vicinity of $X^+ \ ^3\Sigma^- \leftarrow X \ ^2\Pi_{3/2}$, $a^+ \ ^1\Delta \leftarrow X \ ^2\Pi_{3/2}$ and $b^+ \ ^1\Sigma^+ \leftarrow X \ ^2\Pi_{3/2}$ ionizing transitions. Note that the spin-orbit splitting is not taken into account in the calculated values.

ACKNOWLEDGMENTS

This work has received financial support from the French “Agence Nationale de la Recherche” (ANR) under Grant No. ANR-21-CE29-0017 (Project ZEPHIRS). This work was performed on the DESIRS beamline at the SOLEIL synchrotron under Proposals No. 20240446 and 99240021. We are grateful to the whole staff at SOLEIL for smoothly running the facility, in particular the beamline staff Nelson De Oliveira and Jean-François Gil for their precious help in performing the experiments.

DATA AVAILABILITY STATEMENT

Raw data were generated at the SOLEIL Synchrotron large scale facility. Derived data supporting the findings of this study are available from the corresponding author upon reasonable request.

- ¹C. Cabezas, M. Agúndez, N. Marcelino, B. Tercero, Y. Endo, R. Fuentetaja, J. R. Pardo, P. De Vicente, and J. Cernicharo, “Discovery of the elusive thioketenylum, HCCS⁺, in TMC-1,” *Astronomy & Astrophysics* **657**, L4 (2022).
- ²J. Cernicharo, C. Cabezas, M. Agúndez, B. Tercero, J. R. Pardo, N. Marcelino, J. D. Gallego, F. Tercero, J. A. López-Pérez, and P. De Vicente, “TMC-1, the starless core sulfur factory: Discovery of NCS, HCCS, H₂ CCS, H₂ CCCS, and C₄S and detection of C₅S,” *Astronomy & Astrophysics* **648**, L3 (2021).
- ³K. Taniguchi, P. Gorai, and J. C. Tan, “Carbon-chain chemistry in the interstellar medium,” *Astrophysics and Space Science* **369** (2024), 10.1007/s10509-024-04292-9.
- ⁴F. Fontani, C. Ceccarelli, C. Favre, P. Caselli, R. Neri, I. R. Sims, C. Kahane, F. O. Alves, N. Balucani, E. Bianchi, E. Caux, A. Jaber Al-Edhari, A. Lopez-Sepulcre, J. E. Pineda, R. Bachiller, L. Bizzocchi, S. Bottinelli, A. Chacon-Tanarro, R. Choudhury, C. Codella, A. Coutens, F. Dulieu, S. Feng, A. Rimola, P. Hily-Blant, J. Holdship, I. Jimenez-Serra, J. Laas, B. Lefloch, Y. Oya, L. Podio, A. Pon, A. Punanova, D. Quenard, N. Sakai, S. Spezzano, V. Taquet, L. Testi, P. Theulé, P. Ugliengo, C. Vastel, A. I. Vasyunin, S. Viti, S. Yamamoto, and L. Wiesenfeld, “Seeds of Life in Space (SOLIS): I. Carbon-chain growth in the Solar-type protocluster OMC2-FIR4***,” *Astronomy & Astrophysics* **605**, A57 (2017).
- ⁵B. Lefloch, R. Bachiller, C. Ceccarelli, J. Cernicharo, C. Codella, A. Fuente, C. Kahane, A. López-Sepulcre, M. Tafalla, C. Vastel, E. Caux, M. González-García, E. Bianchi, A. Gómez-Ruiz, J. Holdship, E. Mendoza, J. Ospina-Zamudio, L. Podio, D. Quénard, E. Roueff, N. Sakai, S. Viti, S. Yamamoto, K. Yoshida, C. Favre, T. Monfredini, H. M. Quitián-Lara, N. Marcelino, H. M. Boechat-Roberty, and S. Cabrit, “Astrochemical evolution along star formation: overview of the IRAM Large Program ASAI,” *Monthly Notices of the Royal Astronomical Society* **477**, 4792–4809 (2018).

- ⁶K. Taniguchi, M. Saito, T. K. Sridharan, and T. Minamidani, “Survey observations to study chemical evolution from high-mass starless cores to high-mass protostellar objects. ii. HC₃N and N₂H⁺,” *The Astrophysical Journal* **872**, 154 (2019).
- ⁷S. Spezzano, L. Bizzocchi, P. Caselli, J. Harju, and S. Brünken, “Chemical differentiation in a prestellar core traces non-uniform illumination,” *Astronomy & Astrophysics* **592**, L11 (2016).
- ⁸Y. Aikawa, K. Furuya, S. Yamamoto, and N. Sakai, “Chemical variation among protostellar cores: Dependence on prestellar core conditions,” *The Astrophysical Journal* **897**, 110 (2020).
- ⁹J. Kalvāns, “The connection between warm carbon-chain chemistry and interstellar irradiation of star-forming cores,” *The Astrophysical Journal* **910**, 54 (2021).
- ¹⁰I. Fischer and S. T. Pratt, “Photoelectron spectroscopy in molecular physical chemistry,” *Physical Chemistry Chemical Physics* **24**, 1944–1959 (2022).
- ¹¹S.-G. He and D. J. Clouthier, “Is the HCCS radical linear in the excited state?” *The Journal of Chemical Physics* **120**, 8544–8554 (2004).
- ¹²S.-G. He and D. J. Clouthier, “Renner–Teller vibronic analysis for a tetraatomic molecule. I. The effective Hamiltonian and matrix elements,” *The Journal of Chemical Physics* **123**, 014316 (2005).
- ¹³S.-G. He and D. J. Clouthier, “Renner–Teller vibronic analysis for a tetraatomic molecule. II. The ground state of the HCCS free radical,” *The Journal of Chemical Physics* **123**, 014317 (2005).
- ¹⁴S. L. N. G. Krishnamachari and D. A. Ramsay, “The 4114 Å absorption system of the HCCS radical,” *Faraday Discussions of the Chemical Society* **71**, 205–212 (1981).
- ¹⁵S. Krishnamachari and T. Venkitachalam, “A new transient absorption spectrum observed in the flash photolysis of thiophene,” *Chemical Physics Letters* **55**, 116–118 (1978).
- ¹⁶B. Coquart, “Emission spectrum of the HCCS radical,” *Canadian Journal of Physics* **63**, 1362–1371 (1985).
- ¹⁷J. R. Dunlop, J. Karolczak, and D. J. Clouthier, “Pyrolysis jet spectroscopy,” *Chemical Physics Letters* **151**, 362–368 (1988).
- ¹⁸H. Kohguchi, Y. Ohshima, and Y. Endo, “Laser-induced fluorescence spectra and the observation of quantum beats in the $\bar{a}^2\Pi_i - \bar{x}^2\Pi_i$ transition of the HCCS radical,” *Chemical Physics Letters* **254**, 397–402 (1996).
- ¹⁹J. M. Vrtilik, C. A. Gottlieb, E. W. Gottlieb, W. Wang, and P. Thaddeus, “Laboratory Measurement of the Rotational Spectrum of HCCS,” *The Astrophysical Journal* **398**, L73 (1992).
- ²⁰J. Tang and S. Saito, “Microwave spectroscopy of the HCCS and DCCS radicals ($\bar{x}^2\Pi_i$) in excited vibronic states: A study of the Renner–Teller effect,” *The Journal of Chemical Physics* **105**, 8020–8033 (1996).
- ²¹E. Kim, H. Habara, and S. Yamamoto, “Hyperfine Interaction Constants of the HCCS and DCCS Radicals Studied by Fourier Transform Millimeter-Wave Spectroscopy,” *Journal of Molecular Spectroscopy* **212**, 83–88 (2002).
- ²²D. L. Cooper, “Theoretical study of the HCCS radical,” *Chemical Physics Letters* **81**, 479–480 (1981).
- ²³J. R. Flores, “Electronic spectra of SC_nH radicals ($n = 2 - 4$): An ab initio study,” *The Journal of Physical Chemistry B* **107**, 9711–9716 (2003).
- ²⁴J. D. Goddard, “A computational study of the HCCO and HCCS radicals,” *Chemical Physics Letters* **154**, 387–390 (1989).
- ²⁵A. Largo-Cabrero and C. Barrientos, “Theoretical studies of potential astrophysical molecules. the CICC and S&H radicals,” *Chemical Physics Letters* **155** (1989).

This is the author's peer reviewed, accepted manuscript. However, the online version of record will be different from this version once it has been copyedited and typeset.

PLEASE CITE THIS ARTICLE AS DOI: 10.1063/5.0314226

- ²⁶Y. Li and S. Iwata, “Potential energy surfaces of the ground and low-lying states of HCCS and NCS: CASSCF, MRCI and CCSD(T) studies,” *Chemical Physics Letters* **273**, 91–97 (1997).
- ²⁷M. Perić, C. M. Marian, and S. D. Peyerimhoff, “Ab initio study of the vibronic spectrum in the X²Π electronic state of HCCS,” *The Journal of Chemical Physics* **114**, 6086–6099 (2001).
- ²⁸M. Perić and L. Stevanović, “Use of the normal coordinates in variational and perturbative ab initio handling of the vibronic and spin–orbit couplings in π electronic states of linear tetra-atomic molecules,” *International Journal of Quantum Chemistry* **92**, 276–293 (2003).
- ²⁹M. Perić, L. Stevanović, and S. Jerosimić, “Ab initio study of the A²Π–X²Π electronic transition in HCCS,” *The Journal of Chemical Physics* **117**, 4233–4244 (2002).
- ³⁰P. G. Szalay, “Structure and spectra of the thioketenyl (HCCS) radical in its ground and first excited states obtained by *ab initio* coupled-cluster methods,” *The Journal of Chemical Physics* **105**, 2735–2743 (1996).
- ³¹P. G. Szalay and J.-P. Blaudeau, “Theoretical prediction of the spin-orbit splitting in the NCO, NCS, HCCO and HCCS radicals,” *The Journal of Chemical Physics* **106**, 436–437 (1997).
- ³²C. Barrientos and A. Largo, “An ab initio study of C₂S protonation,” *Chemical Physics Letters* **184**, 168–174 (1991).
- ³³C. Puzzarini, “A theoretical investigation on the HCCS radical and its ions,” *Chemical Physics Accurate determination of molecular spectra and structure*, **346**, 45–52 (2008).
- ³⁴M. Michielan, K. Steenbakkars, D. Ascenzi, J. A. Diprose, M. Polásek, S. Brünken, C. Romanzin, B. R. Heazlewood, C. Puzzarini, and V. Richardson, “IR-Action Spectroscopy of the Astrochemically Relevant HCCS+ Cation,” *ACS Earth and Space Chemistry* (2026), 10.1021/acsearthspacechem.5c00248, publisher: American Chemical Society.
- ³⁵X. Tang, G. A. Garcia, J.-F. Gil, and L. Nahon, “Vacuum upgrade and enhanced performances of the double imaging electron/ion coincidence endstation at the vacuum ultraviolet beamline DESIRS,” *Review of Scientific Instruments* **86**, 123108 (2015).
- ³⁶L. Nahon, N. De Oliveira, G. A. Garcia, J.-F. Gil, B. Pilette, O. Marcouillé, B. Lagarde, and F. Polack, “DESIRS: a state-of-the-art VUV beamline featuring high resolution and variable polarization for spectroscopy and dichroism at SOLEIL,” *Journal of Synchrotron Radiation* **19**, 508–520 (2012).
- ³⁷G. A. Garcia, X. Tang, J.-F. Gil, L. Nahon, M. Ward, S. Batut, C. Fittschen, C. A. Taatjes, D. L. Osborn, and J.-C. Loison, “Synchrotron-based double imaging photoelectron/photoion coincidence spectroscopy of radicals produced in a flow tube: OH and OD,” *The Journal of Chemical Physics* **142**, 164201 (2015).
- ³⁸G. A. Garcia, B. K. Cunha de Miranda, M. Tia, S. Daly, and L. Nahon, “DELICIOUS III: A multipurpose double imaging particle coincidence spectrometer for gas phase vacuum ultraviolet photodynamics studies,” *Review of Scientific Instruments* **84**, 053112 (2013).
- ³⁹B. Mercier, M. Compin, C. Prevost, G. Bellec, R. Thissen, O. Dutuit, and L. Nahon, “Experimental and theoretical study of a differentially pumped absorption gas cell used as a low energy-pass filter in the vacuum ultraviolet photon energy range,” *Journal of Vacuum Science & Technology A: Vacuum, Surfaces, and Films* **18**, 2533–2541 (2000).
- ⁴⁰W. A. Chupka, “Factors affecting lifetimes and resolution of Rydberg states observed in zero-electron-kinetic-energy spectroscopy,” *The Journal of Chemical Physics* **98**, 4520–4530 (1993).
- ⁴¹G. A. Garcia, B. Gans, X. Tang, M. Ward, S. Batut, L. Nahon, C. Fittschen, and J.-C. Loison, “Threshold photoelectron spectroscopy of the imidogen radical,” *Journal of Electron Spectroscopy and Related Phenomena* **203**, 25–30 (2015).
- ⁴²S. Gozem and A. I. Krylov, en“*The ezSpectra suite: An easy-to-use toolkit for spectroscopy modeling*,” *WIREs Computational Molecular Science* **12**, e1546 (2022).
- ⁴³M. J. Frisch, G. W. Trucks, H. B. Schlegel, G. E. Scuseria, M. A. Robb, J. R. Cheeseman, G. Scalmani, V. Barone, G. A. Petersson, H. Nakatsuji, X. Li, M. Caricato, A. V. Marenich, J. Bloino, B. G. Janesko, R. Gomperts, B. Mennucci, H. P. Hratchian, J. V. Ortiz, A. F. Izmaylov, J. L. Sonnenberg, D. Williams-Young, F. Ding, F. Lipparini, F. Egidi, J. Goings, B. Peng, A. Petrone, T. Henderson, D. Ranasinghe, V. G. Zakrzewski, J. Gao, N. Rega, G. Zheng, W. Liang, M. Hada, M. Ehara, K. Toyota, R. Fukuda, J. Hasegawa, M. Ishida, T. Nakajima, Y. Honda, O. Kitao, H. Nakai, T. Vreven, K. Throssell, J. A. Montgomery, Jr., J. E. Peralta, F. Ogliaro, M. J. Bearpark, J. J. Heyd, E. N. Brothers, K. N. Kudin, V. N. Staroverov, T. A. Keith, R. Kobayashi, J. Normand, K. Raghavachari, A. P. Rendell, J. C. Burant, S. S. Iyengar, J. Tomasi, M. Cossi, J. M. Millam, M. Klene, C. Adamo, R. Cammi, J. W. Ochterski, R. L. Martin, K. Morokuma, O. Farkas, J. B. Foresman, and D. J. Fox, “Gaussian 16 Revision C.01,” (2016).
- ⁴⁴H.-J. Werner, P. J. Knowles, P. Celani, W. Gyröffy, A. Hesselmann, D. Kats, G. Knizia, A. Köhn, T. Korona, D. Kreplin, R. Lindh, Q. Ma, F. R. Manby, A. Mitrushenkov, G. Rauhut, M. Schütz, K. R. Shamasundar, T. B. Adler, R. D. Amos, S. J. Bennie, A. Bernhardsson, A. Berning, J. A. Black, P. J. Bygrave, R. Cimraglia, D. L. Cooper, D. Coughtrie, M. J. O. Deegan, A. J. Dobbyn, K. Doll, M. Dornbach, F. Eckert, S. Erfort, E. Goll, C. Hampel, G. Hetzer, J. G. Hill, M. Hodges, T. Hrenar, G. Jansen, C. Köppl, C. Kollmar, S. J. R. Lee, Y. Liu, A. W. Lloyd, R. A. Mata, A. J. May, B. Mussard, S. J. McNicholas, W. Meyer, T. F. Miller III, M. E. Mura, A. Nicklass, D. P. O’Neill, P. Palmieri, D. Peng, K. A. Peterson, K. Pflüger, R. Pitzer, I. Polyak, M. Reiher, J. O. Richardson, J. B. Robinson, B. Schröder, M. Schwilk, T. Shiozaki, M. Sibaev, H. Stoll, A. J. Stone, R. Tarroni, T. Thorsteinsson, J. Toulouse, M. Wang, M. Welborn, and B. Ziegler, “Molpro, version , a package of ab initio programs.”
- ⁴⁵J. C. Pouilly, J. P. Schermann, N. Nieuwjaer, F. Lecomte, G. Grégoire, C. Desfrancois, G. A. Garcia, L. Nahon, D. Nandi, L. Poisson, and M. Hochlaf, “Photoionization of 2-pyridone and 2-hydroxypyridine,” *Physical Chemistry Chemical Physics* **12**, 3566 (2010).
- ⁴⁶B. Gans, J. Liévin, P. Halvick, N. L. Chen, S. Boyé-Péronne, S. Hartweg, G. A. Garcia, and J. C. Loison, “Single-photon ionization of SiC in the gas phase: experimental and ab initio characterization of SiC⁺,” *Physical Chemistry Chemical Physics* **25**, 23568–23578 (2023).
- ⁴⁷P.-M. Guyon, R. Spohr, W. A. Chupka, and J. Berkowitz, “Threshold photoelectron spectra of hf, df, and f2,” *The Journal of Chemical Physics* **65**, 1650–1658 (1976).
- ⁴⁸U. Jacovella, B. Ruscic, N. L. Chen, H.-L. Le, S. Boyé-Péronne, S. Hartweg, M. R. Chowdhury, G. A. Garcia, J.-C. Loison, and B. Gans, en“Refining the thermochemical properties of CF, SiF, and their cations by combining photoelectron spectroscopy, quantum chemical calculations, and the Active Thermochemical Tables approach,” *Physical Chemistry Chemical Physics* **25**, 30838–30847 (2023).